A Comparison of Gamma and Lognormal Distributions for Characterizing Dst Variations of Long-lasting Geomagnetic Storms

*M. Chantale Damas[1], Jason Chou[1], Ying Dong[1]

1. Queensborough Community College of the City University of NY (CUNY)

In this study, the Disturbance Storm Time (Dst) profile of long-lasting storms are investigated. Dst variations for the entire duration of storms are approximated using both gamma and lognormal distributions. Profiles of fifty storms were evaluated so far and preliminary analysis showed that the Gamma distribution function may be a better fit overall than the lognormal distribution. Although both distributions tend to approximate the main phase of storms reasonably well, the gamma distribution function tend to approximate the recovery phase much better. Further analysis also shows that the gamma distribution function is also a much better fit than the lognormal distribution for storms caused by ICMEs as opposed to CIR storms. This may due CIR storms long duration recovery phases that can sometimes last days to weeks. This also applies to other storms such as High-Intensity, Long-Duration, Continuous AE Activity (HILDCAA) events with highly fluctuating magnetic fields. Of interest, energy dissipation is also modeled as a diffusion-like process where a 1-D diffusion profile would be equivalent to a Gamma distribution of k = 0.5. Profiles of evaluated storms show this diffusion-like profile suggesting the existence of a diffusion-like process in the energy dissipation in the ring current. More storms are being added to this study to further support our analysis and conclusion. Methods used and results will be discussed

Keywords: Dst, Geomagnetic Storms, Ring Current, ICMEs, CIRs, HILDCAA

惑星間空間磁場B_yが制御する昼間側沿磁力線電流系の起源
Origin of the interplanetary magnetic field B_y-controlled field-aligned current systems on the dayside

*渡辺 正和[1,2]、田中 高史[1]、藤田 茂[3]
*Masakazu Watanabe[1,2], Takashi Tanaka[1], Shigeru Fujita[3]

1. 九州大学国際宇宙天気科学・教育センター、2. 九州大学大学院理学研究院、3. 気象大学校
1. International Center for Space Weather Science and Education, Kyushu University, 2. Graduate School of Science, Kyushu University, 3. Meteorological College

It is well accepted that the field-aligned current systems (FACs) on the dayside are controlled by the dawn-dusk (B_y) component of the interplanetary magnetic field (IMF). We here describe the FAC systems for southward IMF. During IMF B_y-dominated periods, there appears a pair of FAC sheets in the midday sector. When IMF B_y is positive, in the Northern Hemisphere, the equatorward current flows into the ionosphere while the poleward current flows away from the ionosphere. The flow directions are opposite in the Southern Hemisphere. When IMF B_y is negative, the above-mentioned flow directions reverse. Although the morphology is well established, as for the understanding of the magnetospheric sources of those currents, there has been almost no progress in the past two decades. This is because what we can know from observations is very limited. To overcome the difficulty, we performed numerical magnetohydrodynamic simulations using the REPPU (Reproduce Plasma Universe) code recently developed by T. Tanaka. In the talk, we discuss the dynamo processes revealed by the numerical modeling.

キーワード：沿磁力線電流、磁気圏ダイナモ、電磁流体力学
Keywords: field-aligned current, magnetospheric dynamo, magnetohydrodynamics

The influence of IMF cone angle on invariant latitudes of polar region footprints of FACs in the magnetotail: Cluster observation

*Zhengwei Cheng[1], JianKui Shi[1], Jichun Zhang[2], Lynn M Kistler[2]

1. State Key Laboratory of Space Weather, NSSC/CAS, Beijing, 100190, China, 2. Space Science Center, University of New Hampshire, Durham, NH 03824, USA

Field-aligned currents (FACs) were detected by satellites in the 1960s for the first time [*Zmuda et al.*, 1966; *Cummings et al.*, 1967], and they have been observed at both low [*Iijima et al.*, 1978] and high [*Frank et al.*, 1981] altitudes in different regions in geospace. The large scale (from the magnetotail to the ionosphere) FACs are involved in many important physical processes, including field-aligned particle acceleration [*Morooka et al.*, 2004; *Shi et al.*, 2014], magnetic reconnection in the magnetotail [*Ma and Otto,* 2013], development of the substorm current wedge [*Hesse and Birn*, 1991], and auroral activity [*Elphic et al.*, 1998; *Xiong et al.*, 2014].
In solar wind-magnetosphere-ionosphere interactions, the large scale FACs play a crucial role in transferring the solar wind energy and momentum from interplanetary space to low altitude ionosphere. The solar wind and interplanetary magnetic field (IMF) affect the energy transfer process and the associated FACs directly. In the magnetosphere, the importance of the IMF cone angle is not controversial because it is closely concerned with many important physical phenomena. Some studies show that the IMF cone angle effects geomagnetic pulsations (Pc2-5 pulsations) [*Takahashi et al.*, 1984]. *Kavosi and Raeder* [2015] found that the occurrence rate of the Kelvin–Helmholtz waves (KHWs) in the magnetopause increases with the IMF cone angle. Also, the IMF cone angle can control the efficiency of reconnection at the subsolar point [*Scurry et al.*, 1994]. Some authors have suggested that the IMF cone angle can even influence the magnetopause location [*Dušík et al.*, 2010]. In the magnetotail, both IMF cone angle and clock angle are the important factors and have great influences on the FACs. *Cheng et al.* [2013] found the FAC occurrence in the magnetotail increases monotonically with the IMF cone angle. The FAC is a large scale phenomenon in the magnetosphere-ionosphere system. The FACs in the Plasma Sheet Boundary Layers (PSBLs) connected with those in the polar region through the magnetic field lines [*Wild et al.*, 2004] and they are important for the energy flows in the solar wind-magnetosphere-ionosphere system. How the solar wind affects the large scale FACs from the magnetotail to the polar region is still an open question. And no study on the relationship between the IMF cone angle and the invariant latitudes of the FACs in the PSBLs in the magnetotail has been done. This study is focused on the influence of the IMF cone angle on the projection locations of the observed FACs by Cluster in the northern PSBL in the magnetotail. We performed a statistic study of 542 FAC cases observed by the four Cluster spacecraft in the northern hemisphere. The results show that the large FAC (>10 nA/m^2) cases occur at the low ILATs (<71 º) and mainly occur when the IMF cone angle θ >60º, which implies the footprints of the large FACs mainly expand equatorward with large IMF cone angle. The equatorward (poleward) boundary of the FAC footprints decreases (increases) with the IMF cone angle. The equatorward boundary is more responsive to the IMF cone angle. This is the first time a correlation between FAC projected location and IMF cone angle has been determined.

Keywords: FAC in magnetotail, Footprints in polar region, IMF cone angle

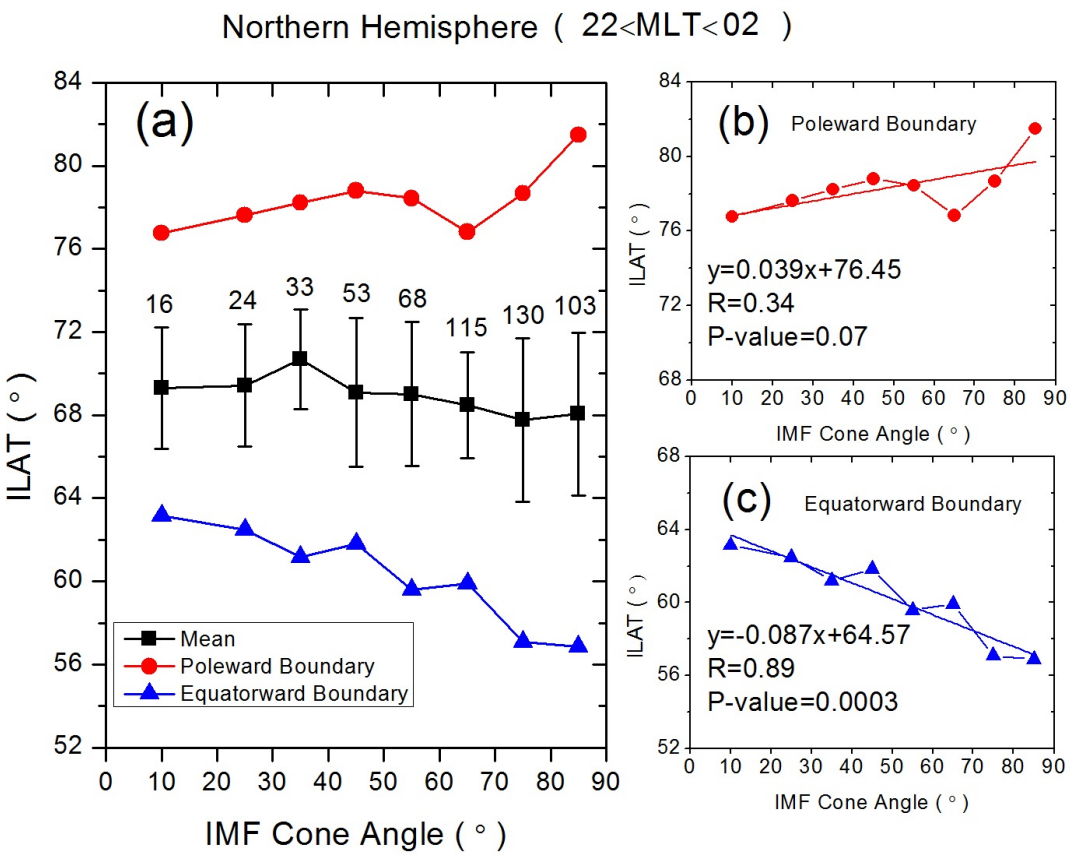

Simulation study of the driving mechanism of the magnetosphere-ionosphere coupling convection

*Shigeru Fujita[1], Takashi Tanaka[2], Masakazu Watanabe[3]

1. Meteorological College, Japan Meteorological Agency, 2. REPPU code institute, 3. Graduate School of Sciences, Kyushu University

The Region 1 field-aligned current (R1FAC) controls the magnetosphere-ionosphere coupling convection. The global MHD simulation reveals that the dynamo of the R1FRC appears in the cusp-mantle region [Tanaka, 1995]. So, in order to elucidate the driving mechanism of the convection, we investigate the link between the solar wind energy and the dynamo of the R1FAC by analyzing the numerical results of the global MHD simulation in the southward IMF condition. This study presents an alternative model of the magnetosphere convection proposed by Dungey (1961). First, the flow motional energy in the solar wind is converted to the thermal energy in the bow shock. This thermal energy is transported to the magnetopause reconnection region. Second, plasma acceleration due to the reconnection in the dayside magnetic field configuration of the null-separator structure does not directly drive the dynamo of the R1FAC. The plasmas in the magnetosheath also contribute to the plasma acceleration. Third, the accelerated plasmas are decelerated when they are transported to the high-latitude magnetosheath next to the cusp. This deceleration invokes the local dynamo. This local dynamo does not drive the R1FAC. This result indicates that the mechanical energy from the solar wind does not directly contribute to driving the R1FAC dynamo. Plasma acceleration in the reconnection region and formation of the local dynamo can be called as the local Dungey process. Fourth, the magnetic energy produced in the local dynamo is transported to and deposited as the thermal energy in the cusp entry region. This mechanism is called as the cusp bridge. Fifth, the thermal energy in the boundary region is accelerated along the field line into the cusp due to the field-aligned pressure gradient. Sixth, the field-aligned accelerated flow is converted to the perpendicular flow in the cusp due to the centrifugal force caused by the field-aligned flow along the bending field line in the cusp. The perpendicular flow goes to the cusp-mantle region. Last, the slow mode expansion mechanism invokes the dynamo of the R1FAC in the cusp-mantle region.

In the talk, we will present how the solar wind condition control the energy transport and conversion from the solar wind to the dynamo region of the R1FAC.

Keywords: magnetospheric convection, MHD simulation , energy conversion

A statistical study of the near-Earth magnetotail evolution duing substorms and pseudosubstorms with themis data

*福井 健人[1]、町田 忍[1]、宮下 幸長[1]、家田 章正[1]、三好 由純[1]、Angelopoulos Vassilis[2]
*Kento Fukui[1], Shinobu Machida[1], Yukinaga Miyashita[1], Akimasa Ieda[1], Yoshizumi Miyoshi[1], Angelopoulos Vassilis[2]

1. 名古屋大学宇宙地球環境研究所、2. カリフォルニア大学ロサンゼルス校
1. Institute for Space-Earth Environmental Research. Nagoya university, 2. University of California, Los Angeles

Substorms and pseudosubstorms (pseudobreakups) are very similar phenomena. In terms of auroral morphology, pseudosubstorms are generally more localized and more short-lived, compared with substorms, and are not accompanied by poleward expansion. We examined auroral development for events from November 2007 through April 2010, using data from THEMIS all-sky imagers. We defined events accompanied and not accompanied by poleward expansion as substorms and pseudosubstorms, respectively. To understand the cause of auroral development, we investigated temporal and spatial development of the near-Earth magnetotail during substorms and pseudosubstorms, based on superposed epoch analysis of THEMIS data. We find that Vx begins to increase at -9.5 >X(GSM)>-11.5 Re around onset for both substorms and pseudosubstorms. This seems to be due to earthward flows caused by magnetic reconnection. Bz also increase around onset at -9.5 >X>-11.5 Re both substorms and pseudosubstorms. The amount and rate of Bz change are larger for substorms than for pseudosubstorms. In the earthward (-7.5 >X>-9.5 Re) and tailward (-11.5 >X>-15.5 Re) regions, Bz increases substantially for substorms, whereas it does not increase very much for pseudosubstorms. These results indicate that dipolarization is weaker for pseudosubstorms than for substorms, and the dipolarization region does not spread extensively for pseudosubstorms. In addition, Brms begins to increase at -6.5>X>-11.5 Re around onset both substorms and pseudosubstorms. The amount of Brms change is larger for substorms than for pseudosubstorms, indicating that waves are strongly induced for substorms. These waves are considered to be caused by instability, and the instability takes place in more for substorms and not in pseudosubstorms. We, therefore, suggest that the occurrence of the instability develops tailward to form the current disruption region and causes auroral poleward expansion. Meanwhile, the plasma and magnetic pressures increase at -6.5 >X>-7.5 Re after onset in association with dipolarization, particularly for substorms. The total pressure (the sum of the plasma and magnetic pressures) prior to the onset is larger in that region for substorms than for pseudosubstorms. At -7.5 >X>-9.5 Re the total pressure hardly differ between substorms and pseudosubstorms. Thus we conclude that the spatial gradient of the total pressure is a key that determines whether the current disruption take place, that is, whether initial activation develops into a substorm or into a subsiding pseudosubstorm.

キーワード：サブストーム
Keywords: substorm

Simultaneous satellite-ground observations of shock triggered substorm expansion

*Jianjun Liu[1], Hongqiao Hu[1], Desheng Han[1]

1. Polar Research Institute of China

Interplanetary (IP) shock encountering the terrestrial magnetosphere can greatly disturb the Earth’s electromagnetic environment and hence intensify the global current system. Here, we examine a distinguishable compression associated auroral event caused by an IP shock sudden impingement to the magnetosphere. We utilize IMAGE satellite auroral imager to obtain the broad global-scale auroral oval over Southern Hemisphere. It is fortunate that part of the nightside poleward branch of the oval was monitored by simultaneous ground-based high temporal-spatial resolution all-sky camera at Antarctic Zhongshan Station (-74.5º magnetic latitude). Satellite imager recorded aurora sudden brightening in pre-midnight just after the IP shock arrival to the magnetosphere. Intensified large-scale aurora experienced interesting azimuthal movement. The poleward and equatorward boundary of the nightside aurora oval featured dramatically enhanced auroral emission with broaden oval width, which presented obvious so-called double auroral oval structure. It is shown that ground-based optical auroral sequential images present prominent westward surge in the poleward branch of the nightside auroral oval, and the westward surge structure shows typical poleward boundary intensifications with periodical signature. This auroral periodical enhancement corresponds well to the geomagnetic variation recorded by the fluxgate magnetometer at Zhongshan station. It is suggested that for substorm triggered by sudden enhanced solar wind dynamic pressure in the precondition of southward IMF, the triggering could occur quite instant after increased dynamic pressure hits on the magnetopause.

Keywords: Interplanetary shock, double auroral oval, substorm expansion

Temporary shrinkage of the near-equatorial tail after the substorm expansion onset

*河野 英昭[1,2]、城谷 一真[1]
*Hideaki Kawano[1,2], Kazuma Shirotani[1]

1. 九州大学大学院理学研究院地球惑星科学部門、2. 九州大学国際宇宙天気科学・教育センター
1. Department of Earth and Planetary Sciences, Kyushu University, 2. International Center for Space Weather Science and Education, Kyushu University

Kawano et al. (2000) presented a case of three recurring substorms, in which the GEOTAIL spacecraft, located in the magnetotail near the equatorial part of the tail magnetopause, temporarily exited the tail and then returned to the tail after the expansion onset for all of the three substorms. The position of GEOTAIL was near (-42, -22, 0) [Re].

They suggested that this phenomenon was caused by the temporary shrinkage of the mid-tail equatorial magnetosphere after the expansion onset, and that the shrinkage was likely to have been caused by the near-Earth neutral line (NENL). That is, as the NENL ejected plasma in the radial direction away from the NENL, it drew in plasma along the line including the NENL toward the NENL, and thus the magnetopause near that line moved inward.

In this paper, we have constructed a database of this kind of events observed by GEOTAIL between Oct. 5, 1993 and Dec. 31, 2002, and examined if the above-stated interpretation is valid. In more detail, we have first identified magnetopause crossings of GEOTAIL based on its observation of the plasma density, temperature, and tailward velocity. We have then selected crossing pairs, i.e., entry-exit pairs and exit-entry pairs, by using the following two criteria: (1) an entry and its paired exit were separated in time by less than three hours; (2) during the four hours consisting of two hours preceding the pair-event start time and two hours following the event end time, GEOTAIL was in the same region (i.e., inside or outside the magnetosphere). We have also identified, as an independent procedure, substorm expansion onsets by using the AL index, and compiled them into another database. Then, for each of the above-identified crossing pairs, we have selected a corresponding substorm onset if the former started less than three hours before or after the latter.

After the above-stated event-selection procedure, we have first compared the starting times of the exit-entry pairs and the substorm expansion onset times. As a result, we have found that the majority of them started after (i.e., not before) the substorm expansion onset, consistent with the temporary-shrinkage interpretation by Kawano et al.

We have also compared the ending times of the entry-exit pairs (which were not studied by Kawano et al.) and the substorm expansion onset times. As a result, we have found that the majority of them ended near the substorm expansion onset time.

More details, including the position dependence of the event occurrence frequency and the time separation between the substorm onset and the event, will be presented at the meeting.

Toward the unified model of substorm

*町田 忍[1]、福井 健人[1]、宮下 幸長[1]、家田 章正[1]
*Shinobu Machida[1], Kento Fukui[1], Yukinaga Miyashita[1], Akimasa Ieda[1]

1. 名古屋大学・宇宙地球環境研究所
1. Institute for Space-Earth Environmental Research, Nagoya University

Numerous models of substorms have been proposed so far, and they are roughly divided into two categories, i.e., an outside-in category that is represented by the NENL model and an inside-out category that is represented by the ballooning instability model. Controversies have been raised for many years over the validity of those models. However, in recent years we have obtained extremely important clues to solve this long-standing issue by separately analyzing THEMIS probe data for substorms and pseudo-substorms. [Fukui et al., 2017]
The key is the plasma pressure in the equatorial region, and in the case of the substorm, it was about 1.4 and 1.2 times larger in the region of X ~ -7 and -8 Re than in the case of the pseudo-substorm. However, no difference was found beyond X~ -10 Re. Therefore, the spatial gradient of the plasma pressure in the region of X ~ -7.5 Re must be a necessary condition for substorm.
An occurrence of abrupt earthward flows originated from the catapult current sheet relaxation and subsequent magnetic reconnection at the NENL just prior to the onset is a common signature for both substorm and pseudo-substorm. Those flows must initiate some instability, possibly the ballooning instability in the earthward side of the flow front.
Substorms do not occur only with the magnetic reconnection. If there is enough plasma pressure gradient, the system can develop into a substorm. Otherwise, it will end up with a pseudo-substorm. We emphasize that both NENL model and the ballooning instability model are partially correct but incomplete, and a true model of substorm can be constructed by combining at least these two.

キーワード：サブストーム、疑似サブストーム、磁気リコネクション、バルーニング不安定
Keywords: substorm, pseudo-substorm, magnetic reconnection, ballooning instability

Evolution process of the theta aurora inferred from global MHD simulations

*三村 恭子[1]、小原 隆博[2]、藤田 茂[3]
*Kyoko Mimura[1], Takahiro Obara[2], Shigeru Fujita[3]

1. 東北大学理学研究科、2. 東北大学　惑星プラズマ・大気研究センター、3. 気象庁気象大学校
1. Faculty of Science,Tohoku University, 2. Planetary Plasma and Atmospheric Research Center, Tohoku University, 3. Meteorological College, Japan Meteorological Agency

The theta aurora sometime appears in the polar cap region when IMF Bz keeps northward.
There are many previous studies, but no unified theory to explain what happens in the ionosphere and magnetosphere during the theta aurora events.

We made MHD simulation by changing IMF By polarity from negative (-4.3nT) to positive (4.3nT) under the northward condition (Bz=4.3nT). Simulation results show there are three stages of the theta aurora evolution. First stage is characterized by the rapid change (within about several minutes) of the anti-clockwise convection to the clockwise one viewed from the north pole in the cusp region of the northern hemisphere. At the same time, upward Region 0 FACs in the post-noon region is exchanged with downward Region 1 FACs in the pre-noon region. Associated with the switch of the FAC polarity in the dayside ionosphere, the dynamo location is also shifted from the post-noon region to the pre-noon region in the dayside magnetosphere. Second stage is characterized by the detachment of high pressure region from the cleft. The detached region move to the high latitude lobe region in the night side and gradually becomes short. This stage lasta about 30 minutes. The high pressure region correspond to the moving front of the changing convection flow. A pair of upward and downward FACs in the ionosphere appears in association with the moving high-pressure region in the magnetosphere. The dynamo appears in the high-pressure region in the magnetosphere as noted below. The closed field line region breaking into the polar cap region associates the pair of the FACs in the ionosphere. We notice that the high-pressure region in the magnetosphere corresponds to the closed field line region. Third stage is given by the extension of the high pressure region to the dayside aurora region. Disturbances in the magnetosphere and in the ionosphere caused by the By change gradually disappear. The FACs become weak, but the closed field line region still beaks into the polar cap. The high-pressure region in the magnetosphere is located in the closed field line region in this stage, too.

It is strongly expected that high pressure region connect to the dynamo region($E \cdot J<0$), we have examined field aligned current signature in high pressure region for three stages. The results demonstrate that pressure region connect to the dynamo region($E \cdot J<0$),consistent with Watanabe et al.(2014). We will report a possible mechanism to generate the dynamo region and its relation to the theta aurora formation in the presentation. It is the final goal of this study to elucidate the state transition mechanism of the magnetosphere-ionosphere compound system caused by the IMF By change.

磁気嵐時のプラズマシート電子内側境界に関する研究
Study of the plasma sheet electron inner boundary during the magnetic storm

*大木 研人[1]、熊本 篤志[1]、加藤 雄人[1]
*Kento Ohki[1], Atsushi Kumamoto[1], Yuto Katoh[1]

1. 東北大学大学院理学研究科地球物理学専攻
1. Department of Geophysics, Graduate School of Science, Tohoku University

The locations of the inner boundary of the plasma sheet electrons during magnetic storm have been analyzed by using the dataset from Time History of Events and Macroscale Interactions during Substorms (THEMIS) satellites.
The dependence of the location of the inner boundary of the plasma sheet electrons on geomagnetic indices such as Kp and AE was investigated in several previous studies [Korth et al., 1999; Jiang et al., 2011]. In addition, several empirical convection electric field model such as Volland-Stern model [Volland, 1973; Stern, 1975], McIlwain's E5D model [McIlwain, 1986], Weimer model [Weimer, 1996], and Matsui Model [Matsui et al., 2013] have been proposed based on the statistical analyses. So, we can trace the expected drift path of the plasma sheet particles in these electric filed models, and compare them with observed locations of the plasma sheet inner boundary.
In this study, we investigated the locations of the inner boundary of the plasma sheet electrons during the magnetic storms by using the electron flux data of 9 keV obtained by Electrostatic Analyzer (ESA) onboard the THEMIS satellites. We determined open/close boundary of the drift paths of plasma sheet electrons in Volland-Stern electric field during the recovery phase of the magnetic storm by performing the test particle simulation, and compared it with the position of the inner edges of the plasma sheet 9-keV electron measured by THEMIS ESA in the same period, because it is a simple macroscopic electric field model depending on slow variation of Kp, and good for the reference to find out the contributions of storm-time electric fields probably with rapid changes and microscopic structures.
We performed the statistical analysis of the positions of the inner edge identified in the recovery phase in the case that differences between the observed plasma sheet electron inner boundary and the open/close boundary of the energetic electron drift path calculated with Volland-Stern convection electric field model [Volland et al., 1973] are less than 0.5 RE. The agreement in these events suggests that the storm-time electric field does not exist around the calculated drift paths. However, as for three of twenty-two events, the calculated drift paths overlap the intense storm-time electric field reported by Nishimura et al. [2008]. In the event on December 20, 2015 around 20:00 MLT (Case-1), the geocentric distance of open/close boundary of the drift path of plasma sheet electrons, Rmodel, is 3.97, and that of the inner edge of the plasma sheet electrons in the magnetic equatorial plane, Robs, is 3.93. We calculated the electric field without the corotation electric field at the plasma sheet electron inner boundary found using Volland-Stern model, and compared it with the storm-time electric field reported by Nishimura et al. [2008]. Ex in the GSM coordinate calculated with Volland-Stern model (Exvs) is 0.23 mV/m while that reported by Nishimura et al. [2008] (Exni) is about -4.00 mV/m. If such large electric field exists on the drift path, the open/close boundary based on Volland-Stern electric field deviates from that of the inner edge of the plasma sheet electrons. From the analysis of another event on October 1, 2012 around midnight (Case-2), Rmodel is 3.50, Robs is 3.18, Exvs is 0.06 mV/m and Exni is about -3.00 mV/m. And as for a event obtained on July 9, 2012 around 20:00 MLT (Case-3), Rmodel is 6.18, Robs is 6.00, Exvs is 0.14 mV/m and Exni is about -1.00 mV/m. In this event, the calculated drift path doesn't overlap

the intense storm-time electric field reported by Nishimura et al. [2008]. From the analysis of another event on February 2, 2015 around 19:00 MLT (Case-4), Rmodel is 7.01, Robs is 7.39, Exvs is 0.07 mV/m and Exni is about -1.00 mV/m.
We focus on Dst index in order to check the above difference. From the analysis of Case-1, Dst index is the smallest in all event and is -155 nT. From the analysis of Case-2, Dst index is the second smallest, and -102 nT. On the other hand, in the event of Case-3 and Case-4, Dst index is -66 and -46 nT. It is considered that plasma sheet ions and electrons distributed in a wide MLT region from the dusk to postmidnight are gathered into the dusk to premidnight sector in the region of enhanced electric field due to the strong ExB drift [Nishimura et al., 2008]. Although the storm-time electric field reported by Nishimura et al. [2008] is the average electric field distributin, from the result obtained on Case-1 - 4, it is considered that the actual storm-time electric field exists more inside during high activities, over 100 nT.

キーワード：磁気嵐、対流電場、リングカレント
Keywords: magnetic storm, convection electric field, ring current

低緯度ー赤道域における磁気急始時の主インパルス振幅の地方時と季節変化

Local time and seasonal variations of the amplitude of the main impulse (MI) of geomagnetic sudden commencements in the low-latitude and equatorial regions

*新堀 淳樹[1]、菊池 崇[1]、荒木 徹[2]、池田 昭大[4]、魚住 禎司[5]、歌田 久司[6]、Commodore Romeo Ho[7]、長妻 努[3]、吉川 顕正[5]
*Atsuki Shinbori[1], Takashi Kikuchi[1], Tohru Araki[2], Akihiro Ikeda[4], Teiji Uozumi[5], Hisashi Utada[6], Commodore Romeo Isidre Ho[7], Tsutomu Nagatsuma[3], Akimasa Yoshikawa[5]

1. 名古屋大学宇宙地球環境研究所、2. 京都大学、3. 情報通信研究機構、4. 鹿児島高等専門学校、5. 九州大学国際宇宙天気科学・教育センター、6. 東京大学地震研究所、7. Hydrography Dept. National Mapping and Resource Information Authority
1. Institute for Space-Earth Environment Research (ISEE), Nagoya University, 2. Kyoto University, 3. National Institute of Information and Communications Technology, 4. National Institute of Technology, Kagoshima College, 5. International Center for Space Weather Science and Education, Kyushu University, 6. Earthquake Research Institute, The University of Tokyo, 7. Hydrography Dept. National Mapping and Resource Information Authority

Local time and seasonal variations of the amplitude of the main impulse (MI) of geomagnetic sudden commencements (SCs) in the equatorial and low-latitude regions (geomagnetic latitude (GMLAT) range: 0 –30 degrees) has been investigated using high time resolution geomagnetic field data for the period 1996 –2009. These geomagnetic field data are provided by the Circum-Pan-Pacific-Magnetometer-Network (CPMN) [Yumoto and the CPMN Group, 2001] and National Institute of Information and Communications Technology (NICT) Space Weather Monitoring (NSWM) [Kikuchi et al., 2008]. In order to identify SC events from January 1996 to 2009, we used the SYM-H index with 1-minute time resolution archived on the web site of World Data Center for Geomagnetism, Kyoto University. In this study, total 6992 SC events were found as a sudden increase of the SYM-H index by more than 5 nT within 10 minutes 1during this period, corresponding to the solar wind dynamic pressure enhancement. The solar wind data are archived on the CDAWeb site. As a result, the local time dependence of the SC amplitude in the low-latitude region (10^{o} < GMLAT < 30^{o}) showed the semi-diurnal variation with two maxima around 10 –14 h (LT) and 22 –1 h (LT) and the two minima around 6 –9 h (LT) and 16 –19 h (LT), respectively. The peak value of the nighttime SC amplitude tended to be equal to or more than that of the daytime amplitude. The minimum value of the SC amplitude in the morning (4 –10 h, LT) tended to be smaller than in the afternoon. This morning-afternoon asymmetry in the SC amplitude is due to a magnetic effect of the two-cell ionospheric currents driven by the MI electric field. The size of the local time variation of the SC amplitude in the low-latitude regions becomes largest in the summer (May –July). During this period, the nighttime SC amplitude tended to be enhanced significantly and was larger than the daytime one. Moreover, the daytime (10 –14 h, LT) SC amplitude at OKI was enhanced significantly near the equinoxes (March and October). The seasonal variation of the SC amplitude at OKI during 10 –14 h (LT) showed a significant decrease during May –October. This depression cannot be explained only by the seasonal variation of the ionospheric conductivity. The local time variation of the SC amplitude in the equatorial region (GMLAT < 10^{o}) clearly showed the equatorial enhancement of the SC amplitude in the daytime (8 –17 h, LT). This enhancement is due to a magnetic effect of the eastward equatorial electrojet driven by a dawn-to-dusk electric field generated during the MI phase of SC. The nighttime enhancement of the SC amplitude as seen in the low-latitude region appeared also in the equatorial region (5.0^{o} < dip latitude < 20.0^{o}). This

result suggests that a magnetic effect caused by a pair of FACs generated during the MI phase of SC extended near the equatorial region. The seasonal variation of the equatorial enhancement of the SC amplitude showed a significant depression by 3 –10 % in the summer (May –July), compared with that in the winter (November –January) in the northern hemisphere. The summer reduction of the SC amplitude can be seen at the GAM and MUT stations located near the dip equator. Moreover, the SC amplitude in the afternoon –evening (14 –21 h, LT) tend to decrease by 10 –30 % during March –September. This summer depression of the SC amplitude appears also at the dip equatorial stations (YAP and PON). From a comparison of the ionospheric conductivity and SC amplitude, it was shown that the decrease of the equatorial enhancement in the morning –evening (8 –21 h, LT) cannot be explained only by the seasonal variation of the ionospheric conductivity. Therefore, the equatorial SC-MI reduction suggests a weakness of a dawn-to-dusk ionospheric electric field during the summer in the northern hemisphere.

キーワード：磁気急始、季節変化、地方時変化、電離圏電気伝導度、赤道域、電離圏電場
Keywords: Geomagnetic sudden commencement, Seasonal variation, Local time variation, Ionospheric conductivity, Equatorial region, Ionospheric electric field

Athabasca University Geophysical and GeoSpace Observatories (AUGO and AUGSO)

*Martin G Connors[1], Ian Schofield[1], Kyle Reiter[1], Kazuo Shiokawa[2], Yuichi Otsuka[2], Mitsunori Ozaki[3], Yoshizumi Miyoshi[2], Ryuho Kataoka[4], Yoshimasa Tanaka[4], Kaori Sakaguchi[12], Reiko Nomura[13], Claudia Martinez-Calderon[5], Jun Chae-Woo[5], Kunihiro Keika[14], Akimasa Ieda[2], Trond Trondsen[6], Devin Wyatt[6], Craig Unick[7], Eric Donovan[7], Brian Jackel[7], Christopher Cully[7], Christopher T Russell[8], Noora Partemies[9], Mikko Syrjaesuo[9], Peter Dalin[10], Mark Zalcik[15], Anthony Tekatch[11], Doug Welch[11]

1. Athabasca University, 2. ISEE, Nagoya University, 3. Kanazawa University, 4. National Institute for Polar Research, 5. Department of Meteorology and Oceanography, UCLA, 6. Keo Scientific Limited, 7. Department of Physics and Astronomy, University of Calgary, 8. IGPP, UCLA, 9. The University Center in Svalbard, 10. Swedish Institute of Space Physics, 11. Unihedron Corporation, 12. National Institute of Information and Communications Technology, 13. ISAS, JAXA, 14. Department of Earth and Planetary Science, University of Tokyo, 15. NLC Can-Am Network

Athabasca University has operated geophysical instruments at AUGO (113º49’ 42” W,54º49’ 42” N) since 1998, and now (since 2012) most are located at AUGSO (113º38’ 40” W,54º36’ 10” N) in a very dark rural location. The geomagnetic latitude of about 61º, less than that of most comprehensive observatories, has led to insight into subauroral and transition region processes. The new AUGSO location has residential facilities capable of hosting up to 9 researchers for campaign style work or installation of equipment. An important feature is fiber optic internet access to both sites, allowing remote operation of instruments. Although most instruments have dedicated, restricted access, sky conditions may be verified, or live auroras may be viewed if they are present, when it is dark, at http://autumn.athabascau.ca/auroracamhd.htm . A magnetometer of the AUTUMN network has operated at the site since 1998, however should not be confused with the nearby NRCan observatory, Meanook. Sample data for the AUTUMN network during the St. Patrick’s Day Storm of 2015 may be found at http://autumn.athabascau.ca/autumnquery.php?year=2015&mon=03&day=17 . Navigation to other pages is easy from there. The AUTUMN sites do not all have the same type of magnetometer, but most take measurements every second, or at 2 Hz, and the data are publicly available and contributed to THEMIS and via there to CDAWeb.

Since 2003, imaging has been done from the Athabasca location. A NASCAM All-Sky Intensified imager was operated from 2004 to 2012, when it was superseded by an EMCCD-based multispectral imager manufactured by Keo Scientific Ltd., at the new, darker site. THEMIS allsky monochrome imagers were tested at Athabasca, and one currently operates there. In 2005, an OMTI multispectral imager was installed along with an H-beta spectrometer. A particularly fruitful field has been that of proton auroras, for which the subauroral location and very dark skies are well suited. Search coil magnetometer detection of Pc1 pulsations coincident with detached proton auroras showed the importance of EMIC waves in causing proton precipitation. More recent coordinated investigations have involved faster imaging so that pulsations in the proton aurora could be detected, as well as VLF emissions coincident with proton auroras and compression events. A riometer was recently installed. Instrument development has also been fostered by AUGSO, most notably the FESO meridian imager which is photomultiplier based with advanced background removal, taking H-beta detection into a new realm of sensitivity and temporal sampling. The combined comprehensive instrumentation is expected to soon be coordinated with in situ measurements by the ERG/Arase satellite, and some preliminary studies involving Van Allen probes have been done.

We continue to operate two sites, with the original one used mainly for instrument testing and support of

a telescope and non-auroral guest instruments. Some specialized studies benefit from having two sites, and we have been very successful in stereo imaging of noctilucent clouds (NLC). Rapid motion of auroral forms has meant less success in stereo studies, but there is great potential.
External instrument development has involved Canadian commercial companies Keo Scientific and Unihedron, both taking advantage of the auroral zone location for optical detection. We are extending our magnetometry and electronics expertise into other domains as well, with most testing done at AUGO.
Both AUGO and AUGSO were funded by the Canada Foundation for Innovation, which also makes a significant contribution to operating costs. The CANARIE computing consortium funded the innovative concept of connection to high speed fiber optic internet at the rural AUGSO site.

Keywords: auroral imaging, proton aurora, observatories, geomagnetism, noctilucent clouds

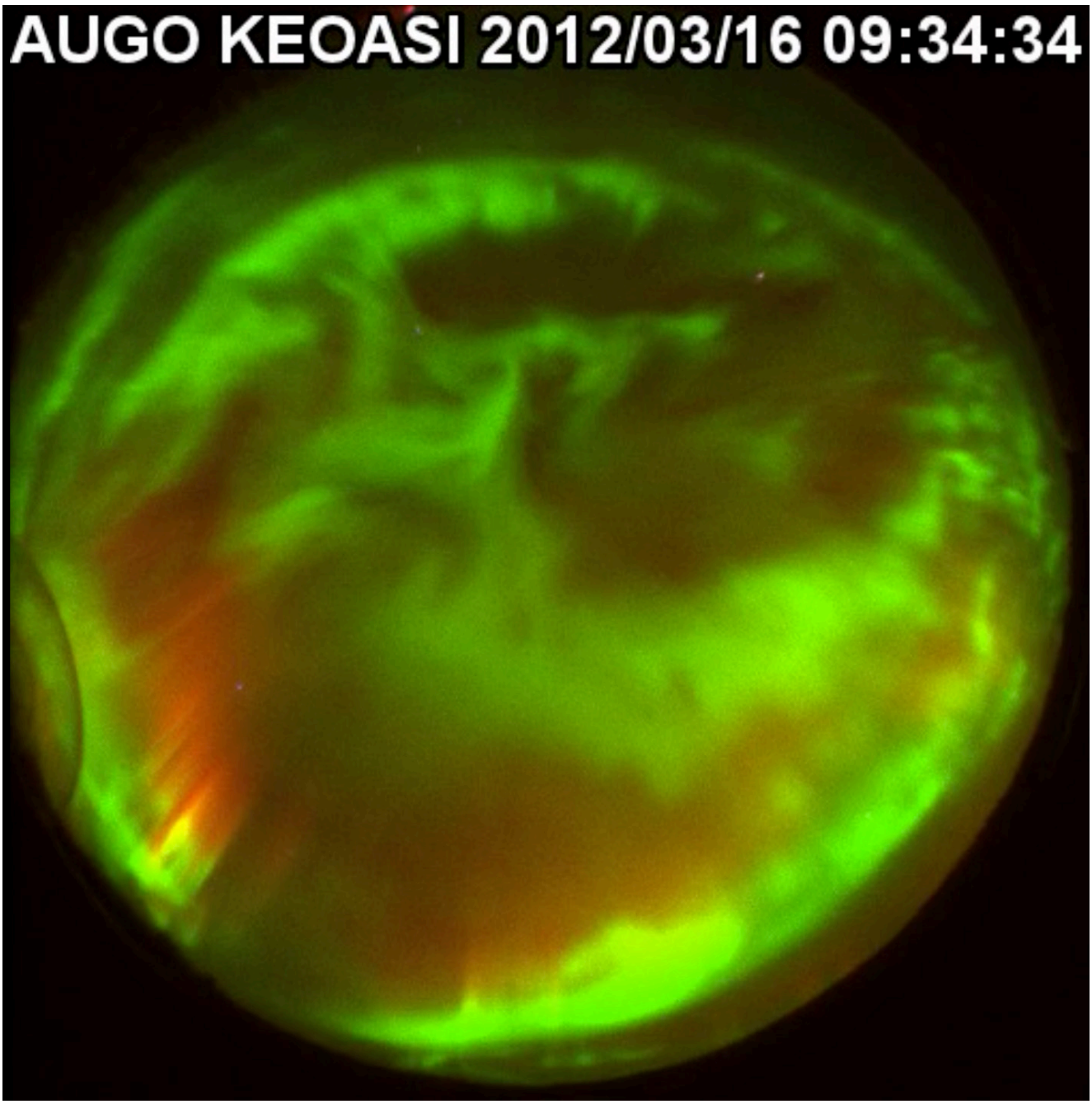

Ionspheric Conductivity Dependence of the Subauroral Polarization Streams Observed by the SuperDARN Hokkaido East HF Radar

*張 玉テイ[1]、西谷 望[1]、堀 智昭[1]
*Yuting Zhang[1], Nozomu Nishitani[1], Tomoaki Hori[1]

1. 名古屋大学
1. Nagoya University

We investigate the characteristics of the subauroral polarization stream (SAPS), with a main focus on the solar zenith angle(SZA) dependence using the Super Dual Auroral Radar Network (SuperDARN) Hokkaido East radar and NOAA POES spacecraft data. In this study, we checked over 2830 days from 2008/1/10 to 2015/12/31 and found 29 SAPS events where the line-of-sight velocity is larger than 150m/s, magnetic local time is 13 to 19 hours and the flow regions are identified to be equatorward of the auroral precipitation region. For each event we examined the SZA using the geographic latitude, longitude and the UT span of SAPS. We identified the lowest possible SZA and lowest illuminated ionospheric altitude for SAPS to be generated, which have not been discussed in detail before. As a result of the statistical analysis, it is found that the SAPS tends to appear when the SZA is larger than 100 degrees, and that the lowest illuminated ionospheric altitude should be higher than about 100km for SAPS to appear. The minimal threshold of the illuminated ionospheric altitude is near the altitude of the peak of Pedersen conductivity. This result suggests that the Pedersen conductivity plays an important role for the generation of SAPS, which is consistent with the previous studies. Results of detailed discussion will be presented.

キーワード：太陽天頂角、磁気圏電離圏カプリング、ペダーセン伝導度、サブオーロラ分極ストリーム、SuperDARN北海道-陸別第一レーダー
Keywords: solar zenith angle, magnetosphere-ionosphere coupling, Pedersen conductivity, sub-auroral polarization stream, SuperDARN Hokkaido East radar

Statistical analysis of ionospheric electric field oscillation associated with Sudden Commencement seen by the SuperDARN radars in the northern hemisphere

*飯田 剛平[1]、西谷 望[1]、堀 智昭[2]
*Iida Kouhei[1], Nozomu Nishitani[1], Tomoaki Hori[2]

1. 名古屋大学宇宙地球環境研究所、2. 東京大学
1. Institute for Space-Earth Environmental Research, Nagoya University, 2. Tokyo University

Sudden Commencement (SC) is observed mainly as a sudden increase of the H-component of geomagnetic field at low latitudes. Past studies showed that it is caused by a sudden compression of the magnetosphere associated with rapid increases of the solar wind dynamic pressure. At middle and high latitudes, SCs cause perturbations associated with twin vortex type ionospheric currents. It was reported that the disturbance of the ionospheric current and the electric field associated with SC consists typically of the Preliminary Impulse (PI) and the Main Impulse (MI). Previous studies reported that some of SC-associated electric field disturbances observed by SuperDARN radars show only the two successive pulses of PI and MI, while some others are accompanied by damped oscillations of the ionospheric electric field lasting for about several tens of minutes to an hour with periods of several minutes. The reason why both types of SC-associated disturbances can occur, however, have not yet been understood well. We examine the cause of the difference between the two kinds of SC events, using SuperDARN radars in the northern hemisphere covering ~40 to 90 degree geomagnetic latitudes. For the analyzed period from January 2011 to December 2015, 244 SC events were identified and 61 events out of them were accompanied by the ionospheric electric field oscillations immediately following MIs, as observed by at least one SuperDARN radar. We contrast 183 events (only PI and MI) with 61 events (oscillation following MIs) and find that the average of magnitude of dynamic pressure change does not seem to be the cause of the difference between two types of disturbance associated with SC events. On the other hand, a detailed analysis on the electric field oscillations shows that some of them exhibit phase differences in latitude and longitude, while the others not. These observations indicate that the ionospheric electric field oscillations sometimes show propagation characteristics. We examine frequencies of the electric field oscillations. We also discuss the magnetic local time (MLT) dependence of the ionospheric electric field oscillations as well as its dependence on spatial displacement of the magnetopause associated with SC.

キーワード：SuperDARN、地磁気急始変化、電離圏電場振動
Keywords: SuperDARN, Sudden Commencement, ionospheric electric field oscillation

Global mapping of ionospheric plasma velocity distributions using spherical elementary current systems based on SuperDARN data

*中野 慎也[1]、堀 智昭[2]、関 華奈子[2]、西谷 望[3]
*Shin'ya Nakano[1], Tomoaki Hori[2], Kanako Seki[2], Nozomu Nishitani[3]

1. 情報・システム研究機構　統計数理研究所、2. 東京大学大学院理学系研究科、3. 名古屋大学宇宙地球環境研究所
1. The Institute of Statistical Mathematics, 2. Graduate School of Science, the University of Tokyo, 3. Institute of Space-Earth Environmental Research, Nagoya University

We have developed a method for estimating the global distribution of ionospheric plasma velocity from the SuperDARN data. The SuperDARN observations have a wide spatial coverage. However, it is difficult to obtain a global ionospheric convection map from the SuperDARN data because individual radars give only line-of-sight components of plasma drift velocity and the data are frequently missing. In our technique, the plasma velocity distribution is represented by a sum of divergence-free spherical elementary current systems, which provides a constraint ensuring the divergence free condition. In this paper, we will demonstrate a preliminary results obtained by our newly developed method.

キーワード：電離圏対流、SuperDARN、SECS
Keywords: ionospheric convection, SuperDARN, spherical elementary current systems

Reconstruction of Plasmaspheric Density Distributions by Applying a Tomography Technique to Jason-1 plasmaspheric TEC Measurements

*Eunsol Kim[1], Yongha Kim[1], Geonhwa Jee[2]

1. Chungnam National University, 2. Korea Polar Research Institute

GPS receiver onboard Jason-1 satellite provides the measurements of plasmaspheric total electron content (pTEC) between the altitudes of Jason-1 and GPS satellites (1,336 and 20,200 km, respectively). We developed a tomography algorithm and applied it to the Jason-1 pTEC data to reconstruct the plasmaspheric density distributions. To invert the observed pTECs into the vertical distribution of plasmaspheric electron density, we adopted a multiplicative algebraic reconstruction technique (MART) with an initial density from *Huang et al. (2004)*. The reconstruction of the plasmaspheric density distribution was performed on Indian ( ), Pacific ( ), and Atlantic ( ) longitudinal planes during the periods of high solar activity ( ) and low geomagnetic activity ( ) from 2002 to 2005. It is found that the reconstructed density distribution displays general climatological characteristics of the plasmasphere. For all three longitudinal sectors, the reconstructed distributions show weak diurnal variations being greater during daytime (09 –15 LT) than nighttime (21 –03 LT). In the Atlantic sector, the reconstructed plasmaspheric density exhibits an annual anomaly (higher density in December than in June), while it was not apparent in the other longitude sectors. By fitting the reconstructed density profiles, we derived the empirical profiles of equatorial plasmaspheric density for four seasons (March, June, September, and December) and for three longitude sectors. The empirical profiles display the diurnal variation and the annual anomaly, and significantly differ from those obtained from other kinds of plasmaspheric measurements.

Keywords: Plasmasphere, Tomography, Total Electron Content, GPS

Latitudinal and Longitudinal Profile of EEJ current during different phases of Solar Cycle

*Nurul Shazana Abdul Hamid[1], Wan Nur Izzaty Ismail[1], Mardina Abdullah[2,3], Akimasa Yoshikawa[4]

1. School of Applied Physics, Faculty of Science and Technology, Universiti Kebangsaan Malaysia, 43600 UKM, Bangi, Selangor, Malaysia, 2. Space Science Centre (ANGKASA), Institute of Climate Change, Universiti Kebangsaan Malaysia, 43600 UKM, Bangi, Selangor, Malaysia, 3. Department of Electrical, Electronic and Systems Engineering, Faculty of Engineering and Built Environment, Universiti Kebangsaan Malaysia, 43600 UKM Bangi, Selangor, Malaysia, 4. International Center for Space Weather Science and Education (ICSWSE), Kyushu University 53, 6-10-1 Hakozaki, Higashi-ku,Fukuoka 812-8581,Japan

Study of equatorial electrojet (EEJ) has always been one of the research interest in ionospheric field. EEJ current is an eastward current that flows within the range of ±3˚ at dip equator. In this study, we attempt to find the latitudinal and longitudinal profile of this ionospheric current. This research is carried on using data from magnetometer network from Magnetic Data Acquisition System (MAGDAS)/ Circum-pan Pacific Magnetometer Network (CPMN), Indian Institute of Geomagnetism (IIG) and International Real- Time Magnetic Observatory Network (INTERMAGNET). The analysis is carried out using geomagnetic northward H component which is later used to calculate the magnetic component of EEJ. In order to correct the latitudinal effect causes by the location of observatories, we applied the normalization technique of observation data. The EEJ latitudinal profile is obtained and it shows that the current started to reverse westward at 5˚ latitude and not more than 10˚ latitude in both hemispheres. On the other hand, the longitudinal profile obtained shows that EEJ is higher in American sector and lowest between African and Indian sector in solar minimum (2008) and inclination phase (2011) of solar cycle. However, in solar maximum (2014), the EEJ current is found to be comparable between American and Southeast Asian sector. Moreover, our result agreed with previous study, showing that the Sq current does not vary with longitude, especially in solar minimum.

Keywords: Equatorial electrojet, Latitudinal profile, Longitudinal profile, Solar cycle

The Sq-current and the Ionospheric Profile Parameters during Solar Minimum

*Nurul Shazana Abdul Hamid[1], Saeed Abioye Bello[2,4], Mardina Abdullah[2,3], Akimasa Yoshikawa[5]

1. School of Applied Physics, Faculty of Science and Technology, Universiti Kebangsaan Malaysia, 43600 UKM, Bangi, Selangor, Malaysia., 2. Space Science Centre (ANGKASA), Institute of Climate Change, Universiti Kebangsaan Malaysia, 43600, UKM Bangi, Selangor, Malaysia, 3. Department of Electrical, Electronic and Systems Engineering, Faculty of Engineering and Built Environment, Universiti Kebangsaan Malaysia, 43600 UKM Bangi, Selangor, Malaysia. , 4. Faculty of Physical Sciences, Department of Physics, University of Ilorin, Nigeria, 5. International Center for Space Weather Science and Education (ICSWSE), Kyushu University 53, 6-10-1 Hakozaki, Higashi-ku, Fukuoka 812-8581, Japan.

The bottomside electron density profile of ionospheric F2-layer can be described by the peak electron density (NmF2), maximum height of F2-layer (hmF2), bottomside thickness (B0) and shape (B1) parameter. We analyze simultaneous quiet days records of these profile parameters with the solar quiet of geomagnetic H-component (SqH) that was obtained from the Peruvian and Ilorin stations respectively during solar minimum. We observe a midday peak in hmF2 and B0 for all the months under study. At the Peruvian station, a post-sunset peak in hmF2 and B0 during the equinoctial month was observed. For all the seasons, we observe peaks in NmF2 during the midday and post-noon periods. The results further show that the variation in SqH current is mainly responsible for that in hmF2 and B0. Both NmF2 and B1 are observed to be less sensitive to the variations in the Sq-current.

Keywords: Ionosphere, Electron density profiles, Sq-current

The correlation analysis of ionospheric characteristics and the geomagnetic Sq fields

*Yu-Jung Chuo[1]

1. Department of Information Technology, Ling Tung University

This study is trying to analysis variations of ionospheric characteristics and geomagnetic Sq fields. Using hourly data of the H and Z components of the geomagnetic observatories from mid-latitudes to equator over the eastern Asian sector in 1999, to calculate the Sq current. The other hand, we calculated the ionospheric total electron content (TEC) by using global positioning satellite system (GPS) data in 1999. In this investigation, we show the daily, seasonal and annual variations of geomagnetic Sq fields and TEC during the solar quiet period in 1999. Meanwhile, this study also collects ionosonde data in Chung-Li at Taiwan to analysis the cross correlation and discussion the possible physics processes for the variation of ionosphere corresponding to the geomagnetic Sq fields.

Keywords: ionospheric dynamo, geomagnetic field, Sq current

オーロラの増光と磁気圏尾部での磁気再結合に伴う高速流の観測
Observation of auroral brightenings and fast plasma flows produced by magnetic reconnection in the magnetotail

*川嶋 貴大[1]、家田 章正[1]、三浦 翼[1]
*Kawashima Takahiro[1], Akimasa Ieda[1], Miura Tsubasa[1]

1. 名古屋大学宇宙地球環境研究所
1. Institute for Space-Earth Environmental Research

サブストームとは、磁気圏全域に及ぶ擾乱によりオーロラ爆発を伴う現象である。このサブストーム開始時には、磁気圏尾部内の地球から20-30地球半径で磁気再結合が発生すると考えられている。磁気再結合が開始すると、地球側では地球向き高速流が、尾部側では尾部向き高速流が発生する。ゆえに、これらの高速流が10地球半径以遠のどこでも観測されるはずである。本研究では、THEMIS衛星5機と地上全天画像を用いて、磁気再結合に伴う高速流の解析を行った。また、尾部向き高速流は磁気再結合のみに伴うものであり、地球向き高速流は磁気再結合に伴うものや磁場の双極子化に伴うものなどがある。そのため、今回は尾部向き高速流が観測されているイベントを解析した。

2009年2月27日06-08 UTにおいて、衛星は尾部側から遠い順に21(THEMIS-1衛星), 18(THEMIS-2衛星), 11Re(THEMIS-3,4,5衛星)の真夜中付近に位置していた。この5機の衛星のfoot-pointsはGillam(磁気緯度66.0度)の全天画像の視野内にあった。Gillamの地上全天画像では、063600 UTに(23.5MLT)でオーロラの増光が始まり、レイ構造が観測された。063600UTにおける衛星観測では、THEMIS-1衛星は、尾部向き高速流を観測した。従って、尾部で磁気再結合がオーロラ増光と同時に生じている。さらに、地球の双極子磁場領域に位置していた衛星3機のうち、2機(THEMIS-3,4衛星)は地球向き高速流を観測した。一方で、3機のうちの残り1機(THEMIS-5衛星)とTHEMIS-2衛星では、地球向き高速流を観測しなかった。この高速流が観測できなかった2機のプラズマベータは、THEMIS-2では1.0, THEMIS-5 では0.1であった。このことから、地球向き高速流が観測できなかった原因として、プラズマシートが薄くなり、衛星の位置がプラズマシート中心領域から外れてしまったことが考えられる。

キーワード：オーロラ、サブストーム、磁気リコネクション
Keywords: aurora, substorm, magnetic reconnection

Auroral intensification in relation to the magnetotail Pi2 and EMIC wave enhancements

*櫻井 亨[1]
*Tohru Sakurai[1]

1. 東海大学
1. Tokai University

This paper presents an important observation for an auroral intensification event in strong relation to the magnetotail Pi 2 and EMIC wave enhancements observed during a substorm event on 04 April 2009. Substorm onset was identified at 08:32 UT with an auroral initial brightening and then an initiation of Pi 2 oscillations at 08:26 UT. About 6 minutes after the auroral intensification occurred at 08:32 UT. The Pi 2 and EMIC wave enhancements were observed at the same time, when THEMIS B satellite encountered the dense plasmaspheric plume at X=~7~8 Re, where was far from the usual location of the plasmapause boundary in the mid-night magneotail. The generation of the EMIC waves was found to be in association with the newly injected westward-drifting ions, oscillating with Pi 2 period. Wave modes appeared with electro-acoustic modes signifying ordinary sound wave, slow mode wave and electromagnetic ion-cyclotron (EMIC) waves at the same time. The frequency of these waves was found to be near He+ gyro-frequency, implying that the presence of heavy ion (He+) might provide new couplings (instabilities) for these EMIC waves. The generation of the EMIC waves might drive the electron heating, suggesting an important candidate for auroral intensification electrons, within the overlap of the ring current and the plasmasplume through some mechanisms such as Coulomb collisions of plasmaspheric electrons with the ring current ions, Landau damping of electromagnetic ion cyclotron waves generated by ring current ions, and/or kinetic Alfven waves in association with the waves. Another important result obtained in this study is a finding of good conjunction between the ground station and the magnetotail from the observation of Pi 2 oscillation period and phase relations between them. The velocity field oscillations observed at the THEMIS-B in the magnetotail showed a same oscillation period of Pi 2 observed on the ground. The velocity field Pi 2 oscillation at the magnetotail leads a quarter cycle for the Pi 2 oscillations observed on the ground. These observations imply that the generation of field-aligned currents (FAC’ s) in association with the velocity field oscillations in the equatorial plane might establish the field-line resonance for these Pi 2 oscillations. Therefore, the present study provides the important role of Pi 2 and EMIC waves for auroral intensification and certifies a good conjugacy between the ground station and the satellite location in the magnetotail.

キーワード：オーロラ、磁気圏、電磁気波動、Pi 2　磁気脈動、イオンサイクロトロン波動、プラズマポーズ
Keywords: aurora, magnetosphere, electro-magnetic waves, Pi 2 magnetic pulsation, electro-magnetic ion cyclotron wave, plasmapause

Comparison of substorm onsets between all-sky images and Pi2 magnetic pulsations.

*三浦 翼[1]、家田 章正[1]、川嶋 貴大[1]
*Miura Tsubasa[1], Akimasa Ieda[1], Kawashima Takahiro[1]

1. 名古屋大学宇宙地球環境研究所
1. Institute for Space-Earth Environmental Research (ISEE), Nagoya University

Substorms are explosive disturbance in the earth’s magnetosphere and ionosphere. Substorm onset are traditionally identified using sudden auroral brightenings or magnetic Pi2 pulsations. These auroral brightenings and Pi2s are believed to occur typically within 1 minutes. On the other hand substorm onset has originally been defined to have two-stage development, i.e., two brightenings. Thus, it is unclear whether the Pi2s correspond to the first or the second brightening. To clarify this association, we compared all-sky images and Pi2 pulsations in Canada, using the data from THEMIS project. As a result, a Pi2 pulsation was observed at 04:36 UT on 29 February 2008. About the same time, an auroral initial brightening (04:33:30 UT) and the poleward expansion (i.e., the second brightening, 04:39:18 UT) were observed in Fort Smith. This result suggests that the Pi2 pulsation can be delayed by a few minutes from the substorm onset, which is originally defined by the auroral initial brightening.

キーワード：地上全天画像、オーロラ爆発
Keywords: All-Sky Images (ASIs), auroral breakup

Simultaneous existence of the cusp aurora and polar cap arcs during northward IMF

*織田 優心[1]、田口 聡[1]、細川 敬祐[2]
*Yushin Oda[1], Satoshi Taguchi[1], Keisuke Hosokawa[2]

1. 京都大学大学院理学研究科、2. 電気通信大学大学院情報理工学研究科
1. Graduate school of science, Kyoto University, 2. Department of Communication Engineering and Informatics, University of Electro-Communications

The cusp aurora for northward IMF is created by the particle precipitation caused by high-latitude reconnection poleward of the cusp. The aurora generally appears at 75 - 80 MLAT in the daytime sector. In this sector the polar cap arcs are also often seen when IMF is northward. In this research we show the spatial and temporal features of the cusp aurora and polar cap arcs by examining events in which both exist simultaneously. We analyzed the 630 nm auroral image data from a highly sensitive all-sky imager at Longyearbyen, Svalbard in Norway, and the precipitating particle and ion drift data from the DMSP spacecraft. The spacecraft data show that lobe convection exists in the daytime sector, and that the cusp electron precipitation and higher-energy electron precipitation occur at different places simultaneously. It is also clear from the all-sky image data that the former and latter produce the cusp aurora and polar cap arcs, respectively. Detailed examination of the all-sky image data obtained immediately before and after the time when whether the observed auroral structures are the cusp proper or polar cap arcs are undoubtedly determined reveals their spatial and temporal features.

キーワード：カスプオーロラ、北向きＩＭＦ、ポーラーキャップアーク
Keywords: cusp aurora, northward IMF, polar cap arcs

Study of polar cap potential saturation using global MHD simulation: Difference between steady and unsteady state

*久保田 康文[1]、長妻 努[1]、田 光江[1]、藤田 茂[2]、中溝 葵[1]、田中 高史[3]
*Yasubumi Kubota[1], Tsutomu Nagatsuma[1], Mitsue Den[1], Shigeru Fujita[2], Aoi Nakamizo[1], Takashi Tanaka[3]

1. 情報通信研究機構、2. 気象大学校、3. 九州大学
1. National Institute of Information and Communications Technology, 2. Meteorological College, 3. Kyushu University

The cross polar cap potential (CPCP) is a value of the convection cycle strength of a solar wind-magnetosphere-ionosphere (SW-M-I) system via Region-1 FAC. CPCP shows an almost linear relationship with the solar wind merging electric field, but it tends to be saturated when the merging electric field becomes large. Siscoe et al. [2002], by using global MHD simulation, suggested that the CPCP basically depends on solar wind electric field, dynamic pressure and ionospheric conductivity. They also suggested that CPCP saturation results from the fact that the solar wind dynamic pressure limits the amount of Region-1 FAC. Their discussion is based on steady state of simulation results, however, in actual cases, solar wind and ionosphere conductivity vary with time and accordingly the state of SW-M-I system should be changed. The purpose of this study is to investigate the cause of the CPCP saturation for time varying condition. In this presentation we will discuss the difference of CPCP saturation between steady and unsteady states.

Possible Formation Mechanism of “Reverse L”-Shaped Transpolar Arc and Associated Ionospheric Flows: A Multi-Event Study

楊 俊[1]、*野和田 基晴[1]、史 全岐[1]、フィアー ロバート[2]、グロコット エイドリアン[3]
Jun Yang[1], *Motoharu Nowada[1], Quan-Qi Shi[1], Robert C. Fear[2], Adrian Grocott[3]

1. 山東大学 威海校 空間科学与物理学学院 空間科学研究院 空間天気物理与探計測研究中心 、2. サウザンプトン大学 天文物理学科 、3. ランカスター大学 物理学科 宇宙惑星物理グループ
1. Center for Space Weather Sciences, Institute of Space Science, School of Space Science and Physics, Shandong University at Weihai, 2. Department of Physics and Astronomy, University of Southampton, 3. Space and Planetary Physics Group, Department of Physics, Lancaster University

We found six events of the interesting shape of Transpolar Arc (TPA) among a large database of IMAGE and POLAR during 5 years between 2000 and 2005. The two events out of six events were observed in northern hemisphere, and the rests were seen in southern hemisphere. A shape of the observed TPA was just like a reversal of the alphabetical letter of “L”, that is, a part of the nightside end of the TPA is “bending” toward the midnight sector. The “bending” polar arc, which is only growing from the nightside main auroral oval, is well-known as “bending arc”, but the TPA, having a bending part at the nightside end, completely grew toward the dayside auroral region. When this “Reverse L”-shaped TPA was observed, the B_z component of the Interplanetary Magnetic Field (IMF) was dominantly northward in almost of cases, and the TPA’s location was determined by the orientation of the IMF-B_y component; the dawn(dusk)side of TPA in northern (southern) hemisphere was seen during the negative B_y component, and under the positive B_y component, the TPA was observed in dusk(dawn)side in northern (southern) hemisphere, which are consistent with the result of a statistical survey for the TPA locations as reported previously. Particularly, on the “Reverse L”-shaped TPA event observed in the northern hemisphere on 22, September, 2000, the SuperDARN radar had detected the ionospheric fast flows, whose range was larger than 0.7 km/s, on the pre-midnight sector of the main auroral oval since, at least, about 2 hours prior to the TPA appearance. Even during the “Reverse L”-shaped TPA brightening, these fast flows persisted. These plasma flows seen in the ionosphere are identified as ionospheric fast flows associated with “Tail Reconnection during IMF Northward Non-substorm Intervals (TRINNIs)”, supporting that this interesting TPA would be formed by nightside magnetic reconnection. However, we also found the case where the TPA separated into the dayside and nightside parts after its appearance, that is, the middle part of the TPA had a “void” structure. These characteristic signatures on the TPA might suggest that formation of “Reverse-L”-shaped TPA would not be addressed by the nightside magnetic reconnection model alone.
We have proceeded further in analysis of these interesting “Reverse L”-shaped TPA events based on both ground- and space-based observations, and supportive global MHD simulations. In this paper, we will discuss the features of ionospheric TRINNI’s flows, whose triggering mechanism is suggestive of nightside magnetic reconnection, and a possible formation mechanism of the “Reverse L”-shaped TPAs based on the results obtained through the detailed analyses.

キーワード：Transpolar Arc、Magnetotail Reconnections、Ionospheric Flows、TRINNIs
Keywords: Transpolar Arc, Magnetotail Reconnections, Ionospheric Flows, TRINNIs

磁気圏双極化によって電離層に流れる電流：事例解析
Field line dipolarization and currents in the ionosphere: A case study

*坂 翁介[1]
*Osuke Saka[1]

1. オフィス　ジオフィジク
1. Office Geophysik

磁気圏双極化（Field line Dipolarization）によって電離層に流れる電流を調べるため、アラスカからラブラドル半島をカバーする地上磁場観測点30ヶ所から得られたデータとアラスカセクターに静止しているロスアラモス衛星のプラズマデータを使い1994年8月10日12:00UTに発生したDipolarizationを対象として調べた。地上観測の結果は以下に示す。

（１）地上磁場鉛直成分の緯度分布に変曲点が現れるが、そこには周囲より強い東あるいは西向き電流が流れている。

（２）開始10－15分の間、最も北の変曲点は急速に68Nから75Nへ移動する。その間、Pi2は40 nTを超える大振幅。

（３）北の変曲点が75Nに達するとその南の変曲点は65Nから68Nへと動く。Pi2の振幅は半減する。この変曲点は西向きジェット電流に相当。

（４）最も南の変曲点の移動は少なく、開始後1時間程度残る。

（５）最も北の変曲点が急速に北へ移動する10－15分の間、onset経度より東側セクターでは東向きに伝播する下向きFACが現れる。

以上の地上観測は静止軌道でのプラズマデータから得られた結果「Field line Dipolarizationは磁力線の地球方向への収縮とそれに直角方向の東への伸展の組み合わせで理解できる」を支持する。

キーワード：磁気圏双極化、電離層電流、電離圏ー磁気圏結合
Keywords: Field line dipolarization, Ionospheric current, M-I coupling

Ionospheric Aflvén resonator observed at low-latitude ground station

*能勢 正仁[1]、上嶋 誠[2]、河合 淳[3]、長谷 英彰[4]
*Masahito Nose[1], Makoto Uyeshima[2], Jun Kawai[3], Hideaki Hase[4]

1. 京都大学大学院理学研究科、2. 東京大学地震研究所、3. 金沢工業大学 先端電子技術応用研究所、4. 地熱技術開発株式会社
1. Graduate School of Science, Kyoto University, 2. Earthquake Prediction Research Center, The University of Tokyo, 3. Applied Electronics Laboratory, Kanazawa Institute of Technology, 4. Geothermal Energy Research & Development Co., Ltd.

The ionospheric Alfvén resonator (IAR) is found in dynamic power spectrum of the geomagnetic field variations as spectral resonance structures in the frequency range 0.1–10 Hz. The first observations of IAR were reported by Belyaev et al. [1989, 1990] by using induction magnetometers installed at a mid-latitude station, Gorkii (L~2.65). Since then, studies of IAR have been focused on events at mid and high latitudes. To date, observations of IAR at low latitude are only made at Crete by Bösinger et al. [2002, 2004] and not sufficient enough to reveal its general characteristics. We therefore installed an induction magnetometer at Muroto, Japan (24.40° geomagnetic latitude, −155.56° geomagnetic longitude), in December 2013 to investigate low latitude IAR in greater detail. Its dipole L value is 1.206 and smaller than that of Crete (L~1.3). Cadence of observations is 64 Hz. We analyze data from the induction magnetometer for the period from 28 December 2013 to 13 August 2016. From the statistical analysis of IAR observed at Muroto, we find that its occurrence probability is (1) dominant during nighttime with a gradual increase from the dusk sector to midnight and a broad maximum at 00–05 LT followed by a sudden decrease at the dawn sector, (2) slightly higher during May through September (in summer and fall), and (3) independent to the Kp index. We also find that (4) IAR at Muroto has frequency separation between the harmonics (Δf) of 0.1–0.5 Hz with a peak at 0.200–0.275 Hz. It has been considered that IAR is caused by Alfvén waves trapped in the ionospheric cavity bounded by the conductive E layer and a steep gradient of Alfvén velocity above the F2 layer. We calculate the resonant frequency and the Q factor of the ionospheric cavity, using analytical equations proposed by Polyakov and Rapoport [1981] with the IRI-2012 and IGRF-12 models. Results of comparison between the observations and the model calculation will be discussed.

オーロラ渦における降下電子エネルギーの時空間変動
Spatiotemporal variation of precipitating electron energy in auroral vortices

*田中 良昌[1]、小川 泰信[1]、門倉 昭[1]、Kauristie Kirsti[2]、Enell Carl-fredrik[3]、Braendstroem Urban[4]、Sergienko Tima[4]、Gustavsson Bjorn[5]、Whiter Daniel[6]、Kozlovsky Alexander[7]、宮岡 宏[1]、Kosch Mike[8]
*Yoshimasa Tanaka[1], Yasunobu Ogawa[1], Akira Kadokura[1], Kirsti Kauristie[2], Carl-fredrik Enell[3], Urban Braendstroem[4], Tima Sergienko[4], Bjorn Gustavsson[5], Daniel Whiter[6], Alexander Kozlovsky[7], Hiroshi Miyaoka[1], Mike Kosch[8]

1. 国立極地研究所、2. フィンランド気象研究所、3. EISCAT科学協会、4. スウェーデン宇宙物理研究所、5. ノルウェー北極大学、6. サウサンプトン大学、7. ソダンキュラ地球物理観測所、8. 南アフリカ国立宇宙機関
1. National Institute of Polar Research, 2. Finnish Meteorological Institute, 3. EISCAT Scientific Association, 4. Swedish Institute of Space Physics, 5. The Arctic University of Norway, 6. University of Southampton, 7. Sodankyla Geophysical Observatory, 8. South African National Space Agency

We investigated dynamic vortex structures in discrete arcs observed by multi-point monochromatic (427.8nm) imagers in Northern Europe at 22:15-22:20 UT on March 14, 2015. We applied auroral computed tomography method to the multiple images taken at 2 second interval by three all-sky EMCCD imagers and at 5 second interval by four wide-view CCD imagers, and reconstructed a 3D distribution of auroral emission and a horizontal 2D distribution of energy of precipitating electrons. The reconstructed 3D distribution of the auroral emission was compared with height profiles of ionospheric electron density along a field line simultaneously observed by EISCAT UHF radar at Tromso, Norway.
The analysis results are summarized as follows. (1) Averaged energy of auroral precipitating electrons was higher around the center of auroral vortices than the other location of the discrete arcs. (2) Total energy flux of precipitating electrons was proportional to the square of the averaged energy. (3) The shape of height profiles of the 427.8nm emission was very similar to that of the electron density profiles. (4) The electron density estimated from the 427.8nm emission by using empirical atmosphere models was about 2.5 to 3 times smaller than observed by EISCAT UHF radar. The result (1) is consistent with the Ohm’s law along a field line, i.e., the field-aligned current (FAC) is proportional to the field-aligned potential difference. If the discrete arcs were caused by electron precipitation from the auroral acceleration region (AAR) where the Ohm’s law is satisfied, the electron energy (proportional to the potential difference) should have been high around the center of vortex where FAC is large. The result (2) strongly supports this inference. As for the item (4), the difference between the electron density estimated from the optical emission and that observed by EISCAT radar may be explained by an uncertainty of some atmospheric parameters derived from empirical models, in particular, an effective recombination coefficient. We discuss the dynamics of the auroral vortices in terms of the magnetosphere –ionosphere coupling.

キーワード：オーロラ渦構造、降下電子エネルギー、トモグラフィ解析、EISCATレーダー、磁気圏電離圏結合
Keywords: auroral vortex structure, precipitating electron energy, tomography analysis, EISCAT radar, magnetosphere - ionosphere coupling

The estimation of spatial structures of magnetospheric plasma by using the data observed by LEO satelites.

*横山 佳弘[1]、家森 俊彦[2]、青山 忠司[1]
*Yoshihiro Yokoyama[1], Toshihiko Iyemori[2], Tadashi Aoyama[1]

1. 京都大学大学院理学研究科地球惑星科学専攻、2. 京都大学大学院理学研究科附属地磁気世界資料解析センター
1. Department of Earth and Planetary Sciences, Graduate School of Science, Kyoto University, 2. Data Analysis Center for Geomagnetism and Space Magnetism,Graduate School of Science, Kyoto University

In the regions of high-beta plasma such as the plasma sheet or the boundary layer in the magnetosphere, it can be expected that the plasma behaves as turbulence due to the effects of various plasma instabilities, non-linear development of Alfven waves, and so on. Satellites in the plasmasheet also have observed the fluctuations in velocity and magnetic field that have the characteristics of fluid turbulence (Borovsky et al. 1997). If the plasmas usually behave as turbulence, the spectrum and their distribution are important for understanding phenomena in the magnetosphere. However, it is almost impossible to have sufficient simultaneous satellite observations that cover the huge magnetospheric domain.

On the other hand, we confirmed that the magnetic fluctuations having period longer than 2s observed by low Earth orbit (LEO) satellites can be regarded as the manifestation of the spatial structure of the field-aligned currents by using the magnetic data obtained by Swarm satellites during December, 2013 when the satellites flew on nearly the same orbits with slight time separations. In addition, the LEO satellites fly through wide range of magnetic latitudes in a short period of time, so, by project- ing their orbits into the magnetosphere, they can scan wide range on the equatorial plane of the magnetosphere. therefore, by projecting these fluctuations onto the equatorial plane of the magnetosphere, i.e., the source regions of field-aligned currents, we try to estimate the distribution of turbulent region and their characteristics there.

We made statical maps of the amplitude of magnetic fluctuations for both quiet(AE<50nT) and disturbed(AE>50nT) conditions. We also made spectral analysis of magnetic fluctuations by MEM and found that there are many peaks in wide frequency range in every spectrum regardless of the geomagnetic conditions, MLTs, and so on.

This result suggests that the magnetospheric plasmas usually behave as turbulence.
In this paper, in addition to the result above, we also discuss the wave-number spectrum in the magnetosphere.

キーワード：SWARM衛星、磁気圏プラズマ
Keywords: SWARM satellite, magnetospheric plasma

Ground-based and magnetospheric observation of auroral finger-like structures using the RBSP-A satellite in the inner magnetosphere

*西 勝輝[1]、塩川 和夫[1]
*Katsuki Nishi[1], Kazuo Shiokawa[1]

1. 名古屋大学宇宙地球環境研究所
1. Institute for Space-Earth Environmental Research, Nagoya University

Auroral emissions are caused by electron precipitation from the magnetosphere along Earth’s magnetic field, and project the magnetospheric plasma dynamics onto the ionosphere. The knowledge of plasma dynamics acquired from investigation of auroral structures is important for future space developments. In our previous research, we reported first conjugate observation event of auroral finger-like structures using the THEMIS GBO cameras and the THEMIS satellites, which was located at radial distance of ~9 Re in the dawnside plasma sheet. The auroral finger-like structures appears in the equatorwardside of the auroral oval in diffuse auroral region, and contribute to the auroral fragmentation into patches mainly during substorm recovery phase. In this study, we searched simultaneous observation events of auroral finger-like structures using the RBSP satellites which has an apogee of 5.8 Re in the inner magnetosphere. The best event which we found is that observed at Gillam, Canada, at ~0900 UT on 14 Nov. 2014. In this event, the footprints of the RBSP-A satellite passed across the auroral finger-like structures several times according to the field-line mapping using the Tsyganenko-01 magnetic field model. We obtained observational facts from this simultaneous observation event as: 1) both electron and ion OMNI fluxes measured by HOPE increase at ~0900 UT as the satellite footprint was getting into the auroral region; 2) electron cyclotron harmonics (Ech) wave activities at ~1 kHz measured by EMFSIS enhanced after 0900 UT; 3) electric field in GSM-Y direction measured by EFW decreases during northward development of the finger-like structures; 4) absolute value of magnetic pressure is almost ten times larger than that of ion thermal pressure; 5) variation of magnetic pressure and ion thermal pressure are seen in various time scales, including ~5 min which is the time scale of crossing of finger-like structures. In the presentation, we will discuss these observations in the context of magnetospheric instabilities that can cause auroral finger-like structures.

キーワード：オーロラ指状構造、RBSP、内部磁気圏
Keywords: auroral finger-like structure, RBSP, inner magnetosphere

Proton aurora dynamics by spectroscopic observations at geomagnetic conjugate points

*高橋 優希[1]、田口 真[1]、門倉 昭[2]
*Yuki Takahashi[1], Makoto Taguchi[1], Akira Kadokura[2]

1. 立教大学、2. 国立極地研究所
1. Rikkyo University, 2. National Institute of Polar Research

Even the brightest proton aurora (486.1nm) is far weaker than electron auroras. When proton aurora is observed, strong emissions from nitrogen molecular ions excited by precipitating electrons may be a contamination. This is the reason why few conjugate observations of proton aurora have been conducted. The studies of proton aurora dynamics using monochromatic imagers in the past could not be definitively justified, because the contamination might remain after subtracting background emission simultaneously observed at a wavelength close to from the image. In this study a spectrum in a wide wavelength range that includes the wavelength of proton aurora is obtained by a proton aurora spectrograph (PAS) in order to precisely eliminate the background emission by electron auroras. PAS has a narrow field-of-view of 180˚ along a geomagnetic meridian, which is accomplished by a variable-width slit placed at the focal plane of an all-sky optics. Light that passes through the slit is converted to a parallel beam and fed into a transmission diffraction grating. Then a space vs wavelength image is projected on a CCD with 1024 × 1024 pixels. Pixel counts are increased by 2 ×2 pixel binning. PAS is designed to observe a wavelength range from 417 nm to 579 nm with a spectral resolution of 2 nm. PAS was installed at the optical observation site at Tjornes in Iceland in early September 2016. Continuous observation started on September 27, 2016, and will end on April 26, 2017. An image was obtained every 3 min with an exposure time of 177 sec from September 27, 2016 to December 8, 2016 and every 1 min with an exposure time of 55 sec from December 12, 2016. The difference in the exposure time is due to increase of sensitivity by updating the CCD camera. The slit width is set to be slightly wider than the designed value, and moreover it is not constant with the zenith angle. Therefore, the slit will be adjusted or replaced to increase the spectral resolution so that the background emission can be perfectly eliminated before the next observation season. An identical system will be developed in early 2017, and will be installed at Syowa Station, where is the geomagnetic conjugate point of Tjornes, during the 2017/2018 summer season. Then conjugate observations of proton aurora will be started from the spring season in 2018.
An example of the spectral data obtained from September 27, 2016 to April 26, 2017 will be introduced and discussed in the presentation.

Development of automatic detection and tracking technique for pulsating aurora

*井上 拓海[1]、井上 智寛[2]、尾崎 光紀[3]、八木谷 聡[3]、今村 幸祐[3]
*Takumi Inoue[1], Tomohiro Inoue[2], Mitsunori Ozaki[3], Satoshi Yagitani[3], Kousuke Imamura[3]

1. 金沢大学 電子情報学類、2. 金沢大学大学院、3. 金沢大学 理工研究域
1. School of Electrical and Computer Engineering, Kanazawa University, 2. Graduate School, Kanazawa University, 3. Institute of Science and Engineering, Kanazawa University

Pulsating aurora is a kind of aurora blinking with several tens of seconds period and having a patchy structure with several to hundreds of kilometers spatial scale. It is difficult to automatically detect pulsating aurora in a video image because the spatial and temporal features of pulsating aurora are complex. Then, statistical analysis would not be enough due to the difficulties. In this study, in order to perform the statistical analysis of pulsating aurora, we have developed an automatic detection and tracking technique for pulsating aurora. Pulsating aurora usually appears simultaneously with diffuse aurora. We apply Low Pass Filter to the brightness variations to reduce the effect of diffuse aurora. Then, we use the Level Set Method to detect the outer shape of pulsating auroral patches. However, the aurora images include a lot of noise so that we are not able to accurately extract pulsating aurora. Here, we evaluated two noise reduction techniques. First is enhancement of the brightness values of aurora images by using a nonlinear function to compress the noise. Second is using the spectral entropy, which is a signal processing method for classifying signal and noise. As a result of evaluation using test data, the first method showed lower error rate of detection (less than 10%) at a signal-to-noise ratio of -5 dB or more in comparison with the second method. We track the motion of pulsating aurora by using a particle tracking technique. We evaluate the accuracy of the tracking technique with a test movie including a simulated auroral patch. The result showed that the tracking error was less than 1 pixel at the signal-to-noise ratio of -10 dB or more.
In this presentation, we will discuss our automatic detection and tracking method for pulsating aurora in detail.

キーワード：脈動オーロラ、画像処理技術、レベルセット法
Keywords: Pulsating aurora, Image processing technique, Level Set Method

EMCCDカメラによる脈動オーロラ変調特性の観測
Characteristics of pulsating aurora modulation observed from high-speed EMCCD camera

*浅野 貴紀[1]、三好 由純[1]、栗田 怜[1]、大山 伸一郎[1]、細川 敬祐[2]、小川 泰信[3]、西山 尚典[3]、町田 忍[1]
*asano takaki[1], Yoshizumi Miyoshi[1], Satoshi Kurita[1], Shin-ichiro Oyama[1], Keisuke Hosokawa[2], Yasunobu Ogawa[3], Takanori Nishiyama[3], Shinobu Machida[1]

1. 名古屋大学宇宙地球環境研究所、2. 電気通信大学大学院情報理工学研究科、3. 国立極地研究所
1. Institute for Space-Earth Environmental Research, ISEE, Nagoya University., 2. Department of Communication Engineering and Informatics, University of Electro-Communications, 3. National Institute of Polar Research

Pulsating aurora (PsA) shows quasi-periodic intensity modulation with a 2 s to 30 s intervals as a main modulation. PsA is mainly observed from the post-midnight to the morning sectors during the recovery phase of substorms. PsA consists of not only main modulations but also internal modulation with a few Hz. We installed multi-EMCCD cameras in Tromso, Finland, Sodankyla, Kevo Finland and Alaska, US. The cameras with RG665 filters observe high-speed phenomena with 100 Hz sampling rate, while the cameras with different filters observe spectrum of PsA with 10 Hz sampling rate. In order to investigate spatio-temporal characteristics of the main modulations as well as internal modulations, we apply PCA (Principal Component Analysis) and FFT to all-sky images of PsA with 100 Hz sampling rate. PCA decomposes into different modes with periods of a few seconds, indicating that localized structure of the main modulation of PsA. The all-sky images at different frequency derived from FFT show that the spatial distribution of PsA depends on the frequency and the internal modulations with high frequency appear in a part of the main modulations. In this presentation, we will report statistical results on these spatio-temporal characteristics of PsA.

キーワード：オーロラ
Keywords: aurora

地上EISCATレーダー・光学多点観測に基づくオメガバンド型脈動オーロラと電離圏D領域電離現象の観測

Coordinated EISCAT and optical network imaging observations of the omega-band type pulsating aurora and electron density enhancement in the D-region ionosphere

近藤 裕菜[1]、*坂野井 健[1]、小川 泰信[2]、田中 良昌[2]、Kauristie Kirsti[3]、Urban Brändström[4]、Gustavsson Björn[5]、鍵谷 将人[1]
Hirona Kondo[1], *Takeshi Sakanoi[1], Yasunobu Ogawa[2], Yoshimasa Tanaka[2], Kirsti Kauristie[3], Brändström Urban[4], Björn Gustavsson[5], Masato Kagitani[1]

1. 東北大学大学院理学研究科惑星プラズマ・大気研究センター、2. 国立極地研究所、3. Finnish Meteorological Institute, Finland、4. Swedish Institute of Space Physics, Sweden、5. UiT The Arctic University of Norway, Tromsø, Norway
1. Planetary Plasma and Atmospheric Research Center,Graduate School of Science,Tohoku University, 2. National Institute Polar Research , 3. Finnish Meteorological Institute, Finland, 4. Swedish Institute of Space Physics, Sweden, 5. UiT The Arctic University of Norway, Tromsø, Norway

今回我々は、地上多点光学観測ならびに EISCAT レーダーにより2016年1月6日と1月13日に観測されたオメガバンド脈動オーロラに伴う低高度電離現象について報告する。

Omega-bandオーロラは朝方高緯度電離圏にしばしば現れる大規模（数十ー数百 km）な波状構造を持つ特徴的なオーロラであり、その中にパッチ状脈動オーロラを有する複雑な構造をしている。脈動オーロラについては、過去の地上観測から 10 keV 以上の比較的高エネルギー降下電子により生成され、100 km 以下の低高度で発光する場合があることが指摘されている。しかしながら、Omega-bandオーロラの発生機構や降下電子のエネルギー特性は依然として観測例が乏しく、ほとんど理解されていない。

本研究では、Omega-bandオーロラの詳細な変動と降下電子エネルギー分布ならびに電離圏応答性を明らかにするために、EISCATレーダーと地上多点光学同時観測データを解析した。

2016年1月6日01:00-02:00 UTと2016年1月13日01:00-02:00 UTにおいて MIRACLE全天イメージャーと Tromsø の EISCAT UHF レーダー同時観測から、Tromsø上空を通過したOmega-bandオーロラの高分解能(空間分解能～10 km以下、時間分解能～10秒以下)データを取得した。このデータに基づき、三角測量を用い、Omega-bandオーロラの427.8 nm及び557.7 nm の発光高度の時間変動を明らかにした。その結果、Omega-bandオーロラの427.8nm発光高度は92-100 kmと低高度であったことが分かった。また、CARD法を用いてOmega-bandオーロラ発生時の降下電子のエネルギー分布を求めた。この結果、2016年1月6日のOmega-bandオーロラは1-100 keVの幅広いエネルギー帯の降下電子によって生成されたことが分かった。一方、2016年1月13日のOmega-bandオーロラの降下電子エネルギー分布は脈動オーロラの降下電子エネルギー分布と同様の15-50 k eV帯であった。このことからOmega-bandオーロラを生成する降下電子エネルギーの特性には複数のタイプあることがわかった。この事実はOmega-bandオーロラ内部の脈動オーロラパッチの生成メカニズムならびに関連磁気圏現象が複数（少なくとも2種類）あることを示唆する。このことからOmega-band内の脈動オーロラを発生させる磁気圏側での波動粒子相互作用には、磁気赤道面近傍のみで共鳴が起きる場合と、磁気赤道面から高緯度側まで共鳴が起こり100keV以上の電子も降り込んでくる場合が考えられる。

また、本研究で開発された発光高度推定手法を定量的に評価した。ディスクリートオーロラの発光高度推定結果や、427.8nmと557.7nmの発光高度差は過去の研究と整合的だった。さらに、三角測量を行う2点間の組み合わせについて、オーロラ空間構造と観測点の位置関係を調べ、3地点観測のうち2地点では高度推定誤差が大きい場合でも他の組み合わせでは比較的正確な高度推定が可能であることが分かった。加えて、高度と三角測量による発光高度の関係を調べた結果、両者には正の相関があることを示した。

キーワード：オメガバンドオーロラ、EISCATレーダー
Keywords: Omega-band type aurora, EISCAT radar

アラスカにおける広角偏光分光装置を用いたオーロラの偏光観測
Observation of auroral polarization using a polarization imaging spectrometer in Alaska

大野 玲央[1]、*坂野井 健[1]、鍵谷 将人[1]
Reo Ono[1], *Takeshi Sakanoi[1], Masato Kagitani[1]

1. 東北大学大学院理学研究科惑星プラズマ・大気研究センター
1. Planetary Plasma and Atmospheric Research Center, Graduate School of Science, Tohoku University

近年の直線偏光子とフォトーメータを組み合わせた極冠域降下電子による酸素原子630nmのオーロラ発光の観測結果から磁力線平行方向に1.9±0.1 %程度の直線偏光が観測された。また、理論的には降下電子エネルギーや位相関数などに対応し、630nm発光が0.6-1.8%程度偏光すると示唆されている[Lilensten et al., 2015]。

本研究では、広視野偏光分光器を用いて、磁気子午線に沿った偏光の仰角分布を長期間にわたって捉えることを目的とし、酸素原子630nmのオーロラの直線偏光の観測を行った。この広視野偏光分光器は、魚眼レンズ、回転するステージに装着したワイヤーグリッド型直線偏光子、VPH透過型回折格子ならびにEMCCD検出器から成り、450nmから710nmの波長範囲で波長分解能2.0nm、視野角130度を有する。偏光子を45度ずつ回転させたときにEMCCDカメラで検出される強度変化から入射光の偏光状態を測定することができる。

偏光計測データには、オーロラ発光の偏光に加え、大気散乱による偏光や、光学系を格納する観測箱のアクリルドーム、魚眼レンズ、回折格子などの機器由来の偏光（以下機器偏光と呼ぶ）の影響をうける。したがって、これらのオーロラ偏光以外の効果を定量的に校正することが本研究の鍵となる。本グループは、2013年よりオーロラ偏光観測を行ってきているが、機器偏光を校正するための装置の不具合や解析方法の未確立により、十分な精度でオーロラ偏光度を見積もることが出来なかった。本研究では、機器偏光の厳密な校正のために、既知の偏光状態を持つ光を入射し、偏光子を回転させながら強度変化を測定する装置を新たに製作した。特に、モーターの回転角の確認を行いながら制御できるよう改良を施した。さらに、この校正光源をもちいて130度の全ての視野方向から入射する光線に対して、機器偏光を厳密に校正する解析方法を開発した。

この広視野偏光分光器と校正光源を2015年11月にアラスカ州ポーカーフラット観測所に設置し、滞在中にこの校正光源装置を用いた厳密な機器偏光の校正データ取得を繰り返し行った。この後、自動運転にて翌2016年3月までオーロラ偏光の連続観測を達成した。

校正データの解析の結果、機器偏光パラメータ（ストークスベクトル）の視野全体の特性を明かにし、偏光度の計測誤差として0.2%程度の十分な精度での校正を達成した。この校正データを用いて、2015年11月19日に観測されたオーロラの偏光解析を行った結果、630nmオーロラの直線偏光度は1.6±0.9%であることが分かった。また、偏光度は磁気子午線に沿って磁北側の低い仰角方向で大きく、仰角が上がるにつれて減少すること、また磁気天頂付近から磁南側のの低い仰角方向いいくに従って再び偏光度が上昇することが明らかになった。また、オーロラ活動度が上昇し発光領域が広がる際に、偏光度が大きくなるといった傾向もみられた。

キーワード：オーロラ、偏光、分光
Keywords: aurora, polarization, spectroscopy

